Defense Threat Reduction Agency
8725 John J. Kingman Road, MS
6201 Fort Belvoir, VA 22060-6201

DTRA-TR-16-23

TECHNICAL REPORT

Radiation Effects on Electronics in Aligned Carbon Nanotube Technology (RadCNT)

February 2019

HDTRA1-10-1-0015

Ivan Sanchez Esqueda et al.

Prepared by:
University of Southern California
3720 S. Flower Street
Los Angeles, CA 90089

DESTRUCTION NOTICE:

Destroy this report when it is no longer needed.
Do not return to sender.

PLEASE NOTIFY THE DEFENSE THREAT REDUCTION AGENCY, ATTN: DTRIAC/ RD-NTF, 8725 JOHN J. KINGMAN ROAD, MS-6201, FT BELVOIR, VA 22060-6201, IF YOUR ADDRESS IS INCORRECT, IF YOU WISH IT DELETED FROM THE DISTRIBUTION LIST, OR IF THE ADDRESSEE IS NO LONGER EMPLOYED BY YOUR ORGANIZATION.

REPORT DOCUMENTATION PAGE

Form Approved
OMB No. 0704-0188

1. REPORT DATE *(DD-MM-YYYY)*	2. REPORT TYPE	3. DATES COVERED *(From - To)*
00/02/2019	Technical Report	22/03/2010 - 21/03/2013

4. TITLE AND SUBTITLE

Radiation Effects on Electronics in Aligned Carbon Nanotube Technology (RadCNT)

5a. CONTRACT NUMBER

5b. GRANT NUMBER

HDTRA1-10-1-0015

5c. PROGRAM ELEMENT NUMBER

6. AUTHOR(S)

Sanchez Esqueda, Ivan
Cress, Cory, D.
Zhou, Chongwu
Che, Yuchi
Fu, Yue
Ahlbin, Jonathan

5d. PROJECT NUMBER

5e. TASK NUMBER

5f. WORK UNIT NUMBER

7. PERFORMING ORGANIZATION NAME(S) AND ADDRESS(ES)

University of Southern California
3720 S. Flower Street
Los Angeles, CA 90089-0001

8. PERFORMING ORGANIZATION REPORT NUMBER

9. SPONSORING/MONITORING AGENCY NAME(S) AND ADDRESS(ES)

Defense Threat Reduction Agency/J4C
8725 John J. Kingman Road, MSC 6201
Fort Belvoir, VA 22060-6201

10. SPONSOR/MONITOR'S ACRONYM(S)

DTRA

11. SPONSOR/MONITOR'S REPORT NUMBER(S)

DTRA-TR-16-23

12. DISTRIBUTION/AVAILABILITY STATEMENT

Distribution Statement A. Approved for public release; distribution is unlimited.

13. SUPPLEMENTARY NOTES

14. ABSTRACT

The main objective of the RadCNT program was the characterization of fundamental mechanisms and charge transport phenomena governing the interactions between ionizing and non-ionizing radiation with carbon-based (nanotube and graphene) field-effect transistors (FETs) devices and integrated circuits (ICs). This effort was supported through the fabrication of aligned single-walled carbon nanotubes (SWCNT) FETs at the University of Southern California's (USC) Nanotechnology Research Laboratory and through the collaboration with the Naval Research Laboratories (NRL) for radiation testing and expertise in radiation effects characterization.

15. SUBJECT TERMS

Total Ionizing Radiation (TID), Carbon-based electronics, Field-effect transistors (FETs), single-walled carbon nanotubes (SWCNTs), graphene, hystersis, charge-trapping, Coulomb scattering, transport, characterization

16. SECURITY CLASSIFICATION OF:			17. LIMITATION OF ABSTRACT	18. NUMBER OF PAGES	19a. NAME OF RESPONSIBLE PERSON
a. REPORT	b. ABSTRACT	c. THIS PAGE			Jacob Calkins
U	U	U	UU	24	19b. TELEPHONE NUMBER *(Include area code)* 571-616-4663

Radiation Effects on Electronics in Aligned Carbon Nanotube Technology (RadCNT)

Final Report

Grant no. HDTRA1-10-1-0015

DTRA Program Manager **Dr. James Reed (james.reed@dtra.mil)**	
Team	
Dr. John Granacki (PI), **Dr. Ivan Sanchez Esqueda** **USC Information Sciences Institute** **3811 N. Fairfax Drive, Suite 200** **Arlington, VA 22203**	**Prof. Chongwu Zhou (co-PI)** **Department of Electrical Engineering** **University of Southern California** **Los Angeles, CA 94305**
Radiation effects modeling, simulation, and testing	**Carbon nanotube transistors and circuit process development and fabrication**
Dr. Cory Cress **Naval Research Lab** **Washington, DC**	**Dr. Michael Fritze (previous PI)** **Dr. Younes Boulghassoul (previous PI)** **USC Information Sciences Institute** **3811 N. Fairfax Drive, Suite 200** **Arlington, VA 22203**
Radiation effects testing and analysis	

Technical Point of Contact:
Dr. J. Granacki (granacki@isi.edu); 703-812-3712
USC Information Sciences Institute
3811 N. Fairfax Drive, Suite 200
Arlington, VA 22203

Administrative Point of Contact
Alan Reyes (alanr@isi.edu); 310-448-8753
USC Information Sciences Institute
4676 Admiralty Way Marina del Rey, Suite 1001
Marina Del Rey, CA 90292

TABLE OF CONTENTS

I. EXECUTIVE SUMMARY

The main objective of the RadCNT program was the characterization of fundamental mechanisms and charge transport phenomena governing the interactions between ionizing and non-ionizing radiation with carbon-based (nanotube and graphene) field-effect transistors (FETs) devices and integrated circuits (ICs). This effort was supported through the fabrication of *aligned* single-walled carbon nanotubes (SWCNT) FETs at the University of Southern California's (USC) Nanotechnology Research Laboratory and through the collaboration with the Naval Research Laboratories (NRL) for radiation testing and expertise in radiation effects characterization.

The RadCNT program concentrated on understanding total ionizing dose (TID) effects on SWCNT and graphene FETs. Several TID experiments with SWCNT and graphene FETs with various gate configurations, dielectric materials and geometries were performed as part of this effort. Well-known mechanisms of radiation-induced degradation in FETs such as oxide charge buildup were confirmed in SWCNT and graphene FETs through *in situ* measurements following radiation exposure. The effects of ionizing radiation on charge-injection mechanisms that cause gate hysteresis in carbon-based electronics were also investigated in this work and demonstrated experimentally for the first time in aligned SWCNT FETs. Recent advances in the fabrication of aligned SWCNT and graphene FETs allowed characterizing electronic transport degradation due to Coulomb scattering from radiation-induced trapped charges near the dielectric interface. Technology computer aided design (TCAD) and physics-based models for describing the electrical properties and radiation response of carbon-based electronics were developed as part of continuing RadCNT effort.

II. RECENT ACCOMPLISHMENTS

A brief description of the accomplishments in the RadCNT program is given here whereas a comprehensive technical description the test structures, experimental setup and procedures and data analysis is provided in section III.

A. Total Ionizing Dose effects in Aligned SWCNT FETs

Total ionizing dose (TID) experiments were performed in view of initial investigations in carbon-based electronics devices (both SWCNT and graphene FETs) that reported a strong dependence of the radiation response on the experimental environment [1-5]. These experiments consisted of Co-60 gamma ray irradiation of aligned single-walled carbon nanotube (SWCNT) field effect transistors (FETs) fabricated with 30 nm Al_2O_3 gate dielectrics and individual back gate electrodes [6]. Results indicate net positive voltage shifts in the transfer (I_d–V_{gs}) characteristics of FETs fabricated *without* a passivation layer masking the surface of the device (i.e., having the SWCNTs exposed to the testing environment). The measured shifts are attributed to contaminants that alter the condition at the surface of the device resulting in an effective *p*-type doping of the nanotubes. These results are consistent with previous investigations where molecular adsorption at the surface of the SWCNTs and/or at the SiO_2 surface near the CNTs results in electron traps that can modulate the nanotube carrier density when irradiated in air [1]. On the other hand, devices fabricated *with* a passivation layer (i.e., 1 μm thick coating of

3612 photoresist) resulted in net negative voltage shifts characteristic of positive charge trapping in the oxide near the SWCNT/oxide interface [6].

In spite of recent advances in the fabrication and performance of SWCNT FETs, the existence of substantial gate hysteresis in the transfer characteristics has continued to be a significant limitation for the development of carbon-based electronics and for the analysis of their electrical properties [7-13]. To overcome these limitations we have thoroughly investigated the physical mechanisms, characterization techniques and the radiation response of gate hysteresis in aligned SWCNT FETs [13]. Based on this investigation, pulsed and standard (*i.e.*, non-pulsed) I_d-V_{gs} measurement techniques were developed for analyzing the combined effects of hysteresis and radiation-induced degradation. These measurements support a dynamic screening model based on charge injection mechanisms for describing gate hysteresis. The impact of ionizing radiation on charge injection mechanisms was established experimentally through *in situ* measurements of SWCNT FETs performed under static vacuum. Extractions of hysteresis width (h) indicated an increase of more than 20 % after 1 Mrad(SiO_2) of TID exposure for worst-case conditions. This increase in h indicates a larger contribution from charge injection mechanisms as a function of ionizing radiation exposure. TCAD simulations were used to investigate the combined effect of hysteresis and radiation-induced degradation and to demonstrate its dependence on trap density, carrier lifetime and energy distribution. The measurements of hysteresis as a function of increasing radiation exposure and gate voltage (V_g) sweep range reveal non-uniform buildup in the energy distribution of trapping centers near the SWCNT/dielectric interface. The results are consistent with extensive studies on classical bulk semiconductor/oxide interfaces (e.g., in the Si/SiO_2 system). As we discuss in [14], the analysis is supported with self-consistent calculations of surface potential and carrier densities in the SWCNTs and generation-recombination statistics at the radiation-induced trapping centers. Calculations of surface potential and carrier densities incorporate the SWCNT band structure, density of states and quantum capacitance allowing investigating the dependence of charge injection mechanisms on SWCNT diameter and chirality. Additionally, the mitigation of gate hysteresis is investigated using novel SWCNT device configurations and processing steps as part of the RadCNT program. The techniques for hysteresis mitigation are further described in subsection C.

As summarized above, the *extrinsic* effects of ionizing radiation exposure on aligned SWCNT FETs (i.e., voltage shifts and increased gate hysteresis) have been demonstrated through measurements of degraded (I_d-V_{gs}) characteristics. Furthermore, extractions of drain conductance and carrier mobility degradation as a function of TID have determined the effects on the transport properties of carbon-based electronics [15]. In [16] we present an approach for describing the impact of radiation-induced defects on the transport properties of carbon-based nanoscale transistors that operate near the ballistic limit. This approach accounts for increased scattering due to the formation of structural defects in the channel of the transistor caused by energetic particle radiation and/or charged impurities that result from ionizing radiation effects in oxide regions near the channel.

B. Total Ionizing Dose effects in Graphene FETs

TID experiments on graphene FETs were also performed as part of the RadCNT program. Graphene FETs fabricated by chemical vapor deposition (CVD) and transferred onto trimethylsiloxy (TMS)-passivated SiO_2Si substrates [17] and epitaxial graphene on

6H-SiC substrates (via Si sublimation) [18] had similar TID responses. In both cases radiation exposure resulted in positive oxide trapped charges near the graphene/oxide interface as manifested by negative voltage shifts in the I_d-V_{gs} characteristics, degradation of carrier mobilities and increased minimum conductivity. A semi-empirical approach for modeling the radiation-induced degradation effective carrier mobility in graphene FETs was also developed as part of this effort [19]. The modeling approach describes Coulomb and short-range scattering based on calculations of charge and electric field that incorporate radiation-induced oxide trapped charges. The model can correctly describe the transition of the dominant scattering mechanism as a function of effective vertical field and oxide trapped charge density. The proposed modeling approach was verified with experimental data from Co-60 irradiation of graphene FETs resulting in excellent qualitative agreement [19].

The procedures, analysis techniques and modeling approach developed in the RadCNT program for studying the effects of radiation-induced oxide trapped charges on the transport properties of graphene FETs can be extended to graphene transport on other dielectric materials. These methods potentially provide a means for systematically studying the properties of the interface between carbon nanomaterials (e.g., graphene, SWCNT) and the substrate (e.g., oxides) [15].

C. Technology Development and Device Optimization

Significant progress has been made during the past three years at USC's Nanotechnology Research Laboratory to address serious impediments for the reliable implementation of SWCNT-based electronics particularly in the assembly and purity of the synthesized CNTs. For instance, a combined synthesis process of *aligned* nanotubes and stacked transfer technology has been developed to achieve a density of 60 CNTs/μm, which can provide electrical performance better than state-of-art Si transistors [20]. In addition, to address the problem of coexistence of metallic and semiconducting nanotubes, synthesis of predominantly semiconducting nanotubes (~90%) by using isopropanol alcohol as the feedstock has been demonstrated [21]. Further control of the chirality of synthesized nanotubes, and therefore the percentage of semiconducting tubes, has been obtained using pre-separated chirality-pure carbon nanotubes as seeds for "nanotube cloning" based synthesis [22]. Moreover, the fabrication of hysteresis-free, self-aligned "T-gate" SWCNT FETs with ultra-thin Al_2O_3 gate dielectrics has been achieved recently resulting in superior performance and quasi-ballistic regime operation [23].

As mentioned previously, the prominent gate hysteresis effect has been a serious impediment for the implementation of carbon-based electronics as well as for the study of the electronic properties, performance and radiation response as a result of the associated threshold voltage instability. The recent progress in hysteresis mitigation obtained by utilizing self-aligned T-gate structures and ultra thin gate oxides is therefore significant not only for the technological advancement of carbon-based electronics but also for allowing a comprehensive and accurate evaluation of the radiation effects on the electrical performance of SWCNT and graphene FETs. The self-aligned processing of the aforementioned T-gate structures provides complete isolation of the SWCNTs and allows utilizing a thin gate dielectric with improved interface quality resulting in negligible hysteresis.

N-type SWCNT FETs were achieved using low workfunction metals such as Gd as

source/drain contacts enabling the fabrication of complementary (i.e., CMOS) logic circuits [24]. The recent progress in fabrication and the unique channel characteristics and gate topology of the *aligned* SWCNT FETs makes them ideal research vehicles for the basic investigation of radiation effects in SWCNT-based technology.

III. TEST STRUCTURES AND EXPERIMENTAL SETUP

This section provides a brief description of the fabrication steps of the aligned SWCNT and graphene FET test structures used for the radiation studies in the RadCNT program. Shown in Fig. 1 is an illustration of the full wafer processing of aligned nanotubes (including synthesis and transfer) and device fabrication [24]. Wafer-scale synthesis of aligned SWCNT in quartz substrates is accomplished through a meticulous temperature control during the growth process (Fig. 1a). As illustrated in Figs. 1b-1d, a facile transfer method based on depositing a thin gold film (~ 100 nm) and using thermal tape peel-off allows transferring the CNT into the target substrate (e.g., Si/SiO2 substrate). Removing the gold film using gold etchant results in an array of massively aligned SWCNTs on the target substrate (Fig. 1e). Device fabrication follows standard silicon CMOS technology such as projection photolithography, metal patterning and dielectric deposition (Fig. 1f). This process flow can result in common back-gated and/or individually top-gated SWCNT FET test structures. Alternatively, patterning gate electrodes and depositing a gate dielectric layer prior to the transferring the SWCNTs yields individually back-gated aligned SWCNT FETs with high-κ dielectrics (e.g., HfO_2, Al_2O_3, etc.) [2]. Shown in Fig. 2 are schematic diagrams of two SWCNT FET test structure configurations used in the RadCNT program.

Shown in Fig. 3a is the irradiation vessel used for *in situ* measurements and TID exposure at the naval research laboratories (NRL). The irradiation vessel allows the required connections for electrical characterization of the SWCNT FETs and for biasing during radiation exposure. Irradiation and measurements can be done in air, with flowing ultra high purity (UHP) N_2 or under static vacuum. TID experiments conducted at NRL consisted in step-stress Co-60 gamma ray irradiation up to various total dose levels. Shown in Fig. 3b is the Co-60 irradiation facility at NRL. The irradiation facility is comprised of a 25000 Ci Co-60 source house at the bottom of a 10 ft. pool. The irradiation vessel (Fig. 3a) is lowered into the Co-60 source while using a plastic snorkel to make electrical connections to a Keithley 4200-SCS parameter analyzer. The dose rate was approximately 990 rad(Si)/s for all the experiments discussed here unless otherwise stated.

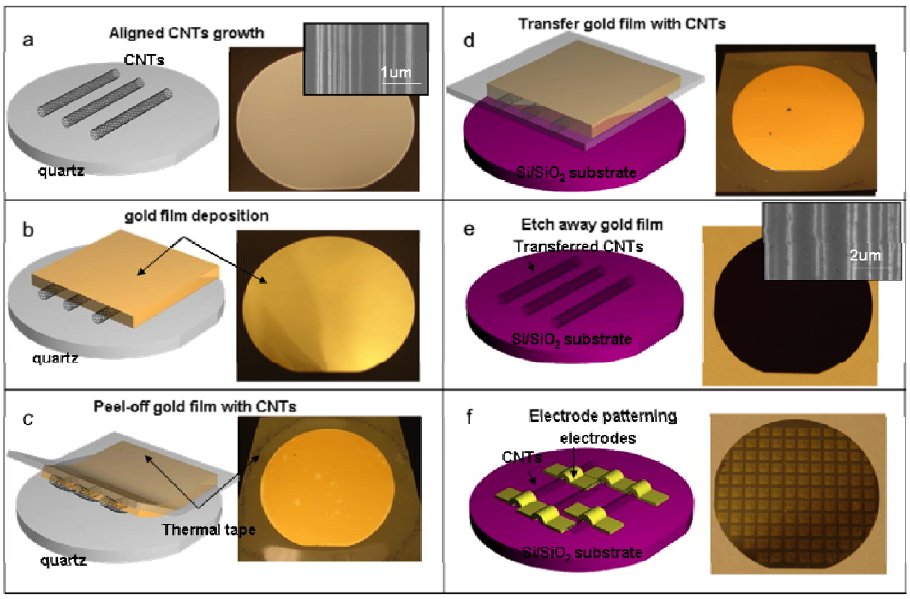

Fig. 1. (a) Schematic diagram and photograph of full wafer synthesis of aligned nanotubes on a 4 in. quartz wafer, (b) gold film deposition, (c) peeling off the gold film with nanotubes, (d) transfer of the gold film with the nanotubes onto a Si/SiO2 substrate, (e) etching away the gold film and (f) device fabrication on the transferred nanotube arrays.

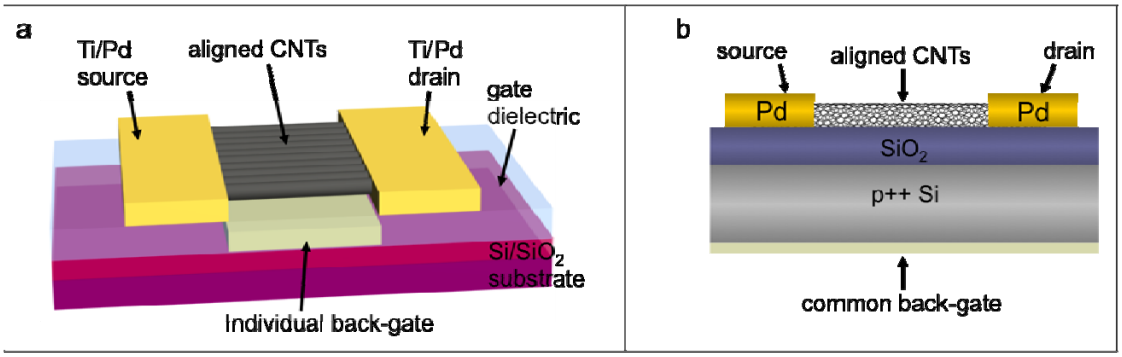

Fig. 2. Schematic diagrams of SWCTN FET test structures used in the RadCNT program. (a) Individually back-gated aligned SWCNT FET with high-k gate dielectric. (b) Common back-gated aligned SWCNT FET with SiO_2 gate dielectric.

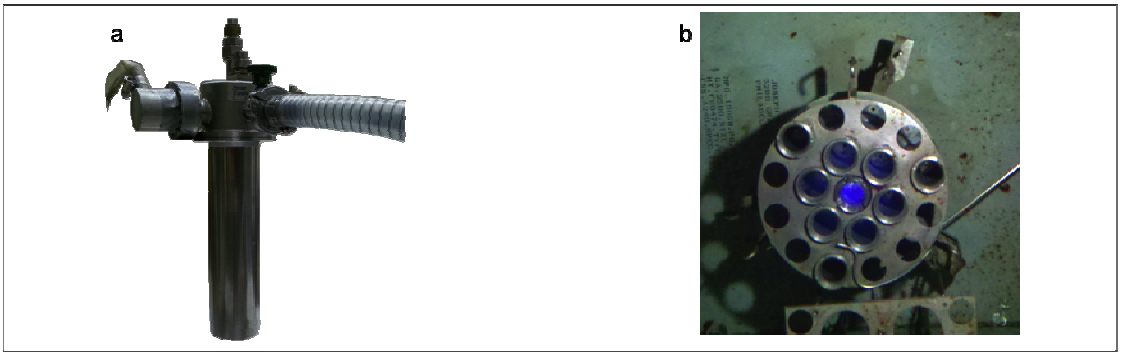

Fig. 3. Irradiation vessel used as the vacuum chamber and (b) irradiation chamber in the Co-60 pool at NRL.

IV. RESULTS

A. Experimental Environment (Aligned SWCNT FETs)

A summary of results from TID experiments on SWCNT and graphene FETs is given in this section. The results shown in this section of the report consist of reduced data obtained from analysis and/or extractions based on the degraded *I-V* characteristics of the transistor test structures following radiation exposure. Preliminary experiments consisted of *in situ* characterization of the total dose response of individually back-gated aligned SWCNT FETs with 30 nm Al_2O_3 gate dielectrics (see Fig. 2a). These experiments were performed for devices with and without a passivation layer that shield the CNTs to the experimental ambient conditions. The purpose of these experiments was to confirm the results observed in random network (RN)-based CNT FETs where devices irradiated in air and under vacuum resulted in opposite shifts in the *I-V* characteristics [1]. Indeed, the threshold voltage shifts (ΔV_{th}) shown in Fig. 4a increase negatively as a function of TID for the passivated devices (consistent with positive charge trapping in the oxide), but are net positive for the unpassivated ones [6]. The positive ΔV_{th} observed for the unpassivated devices has been attributed to *p*-type doping caused by water and oxygen adsorption at the surface of the SWCNTs or by electron traps bound to silanol groups at the SiO_2 surface near the CNTs. Additionally, as shown in Fig. 4b, the measured effects of ionizing radiation on carrier mobility (i.e., peak field effect mobility) is opposite for devices with and without passivation.

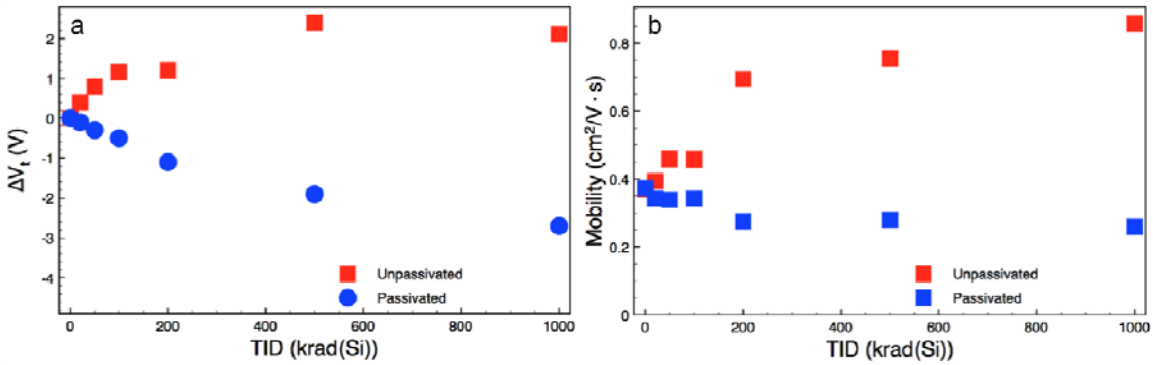

Fig. 4. Comparison of (a) radiation-induced threshold voltage shifts (ΔV_{th}) and (b) mobility degradation plotted as a function of TID for passivated and unpassivated SWCNT FETs

B. TID and Gate Hysteresis (Aligned SWCNT FETs)

Electrical characterization from the preliminary experiments revealed significant gate hysteresis in the transfer characteristics of the aligned SWCNT FETs. In many recent studies it has been assumed that the mechanisms causing gate hysteresis are not affected by ionizing radiation and can be investigated independently. An important aspect of the RadCNT program has been to identify these mechanisms and study their radiation response. Charge injection from the CNTs to the CNT/oxide interface has been identified as a significant contributor to gate hysteresis. As part of this effort we have experimentally demonstrated and analyzed the dependence of charge-injection mechanisms to ionizing radiation. We experimentally verified charge injection via near-interfacial donor- and acceptor-like traps through measurements of hysteresis in dual V_g sweeps as a function of the sweep range (V_{gmax}). In these experiments the forward sweep

ranged from $-V_{gmax}$ to V_{gmax} and the reverse sweep from V_{gmax} to $-V_{gmax}$ where V_{gmax} = 2, 4, 6, 8 and 10 V. Shown in Fig. 5a are the obtained drain current (I_d) vs. gate-to-source voltage (V_{gs}) characteristics for a SWCNT FET with W = 200 µm, L = 2 µm and using V_{ds} = –0.1 V. The inset in Fig. 5a plots the relationship between V_{gmax} and the hysteresis width (h) defined as the difference in V_g at $I_d = I_0$ for the reverse and forward V_g sweeps. For the measurements shown here I_0 = 100 µA (e.g., the red arrow in Fig. 5a shows the extraction of h for V_{gmax} = 6 V). The results in Fig. 5 show an increase in h with V_{gmax} attributed larger carrier densities in the SWCNTs contributing to charge injection resulting in accumulation of trapped charges. Additionally, negative voltage shifts in the forward sweep and positive voltage shifts in the reverse sweep with increasing V_{gmax} are indicative of charge contribution from both donor-like and acceptor-like traps. Donor-like traps are positively charged when ionized (empty) and acceptor-like traps are negatively charged when ionized (occupied).

Fig. 5b plots the I_d-V_{gs} characteristics as a function of total ionizing dose (TID) for a fixed sweep range of V_{gmax} = 8 V. In addition to increased h, the results reveal a reduction in transconductance consistent with mobility degradation as a function of TID. At every dose level the hysteresis width h is extracted from the forward and reverse V_g sweeps for increasing V_{gmax}. Fig. 6a plots h as a function of V_{gmax} for increasing levels of TID. The relationship between h and V_{gmax} depends on the energy distribution of the trapping centers since the ionization probability for traps with energy levels closer to the band edges increases with V_{gmax}. In other words, V_{gmax} modulates the energy levels that area accessible for trapping. Therefore, the relationship between h and V_{gmax} for increasing TID provides a way to characterize the energy distribution of the radiation-induced trap buildup. Fig. 6b plots the change in h (i.e., $\Delta h = h - h_0$ where h_0 is the hysteresis width prior to irradiation) as a function of total ionizing dose (TID) and for increasing V_{gmax}. These results indicate an increase in h with TID that is more significant for larger V_{gmax}.

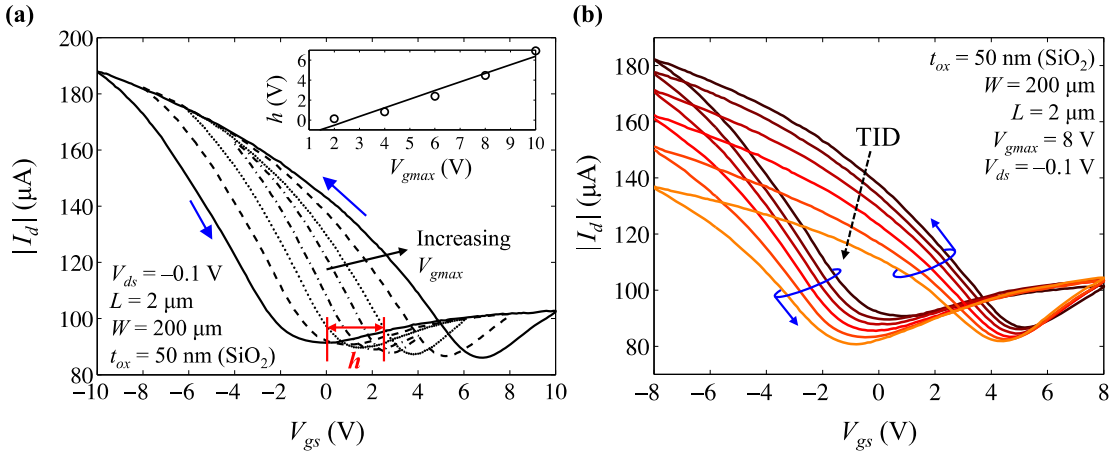

Fig. 5. (a) Drain current (I_d) vs. gate-to-source voltage (V_{gs}) characteristics for a SWCNT FET with W = 200 □m, L = 2 □m and using V_{ds} = –0.1 V and increasing the gate-voltage sweep range (V_{gmax}). The inset plots the relationship between V_{gmax} and the hysteresis width (h) [13]. (b) I_d-V_{gs} characteristics as a function of TID for fixed V_{gmax} [13].

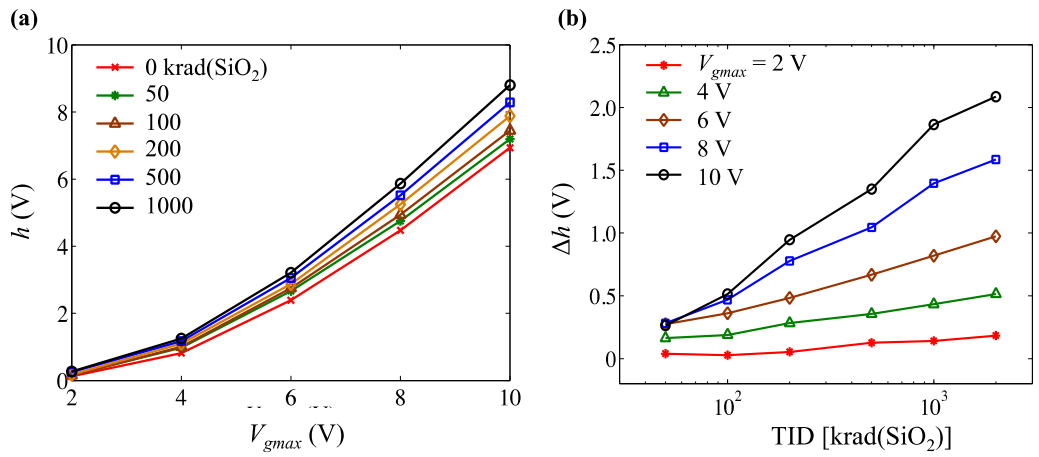

Fig. 6. (a) Hysteresis width (h) plotted as a function of V_{gmax} for increasing levels of total ionizing dose (TID) [13]. (b) Change in h (i.e., $\Delta h = h - h_0$) as a function of total ionizing dose (TID) and for increasing V_{gmax} [13].

As described in [14], the effects of charge injection on gate hysteresis can be described by the generation-recombination of carriers in the nanotube array via the interaction with near-interfacial traps in the gate dielectric. Self-consistent calculations of surface-potential, carrier density and trapped charge are used to describe hysteresis as a function of ionizing radiation exposure. The calculations demonstrate the relationship between hysteresis width and trap density resulting in a stronger dependence on V_{gmax} for non-uniform D_T energy distributions. Good agreement between theory and experimental data is obtained with a "U-shaped" non-uniform energy distribution of D_T located within 15 nm from the SWCNT/SiO_2 interface. Shown in Fig. 7a is the simulated non-uniform distribution of interface traps and the buildup as a function of total ionizing dose. Calculations of hysteresis width as a function of V_{gmax} for the simulated D_T are shown in Fig. 7b. Finally, the comparison with experimental data is given for the increase in hysteresis width (Δh) as a function of TID for various values of V_{gmax} in Fig. 7c with good qualitative agreement.

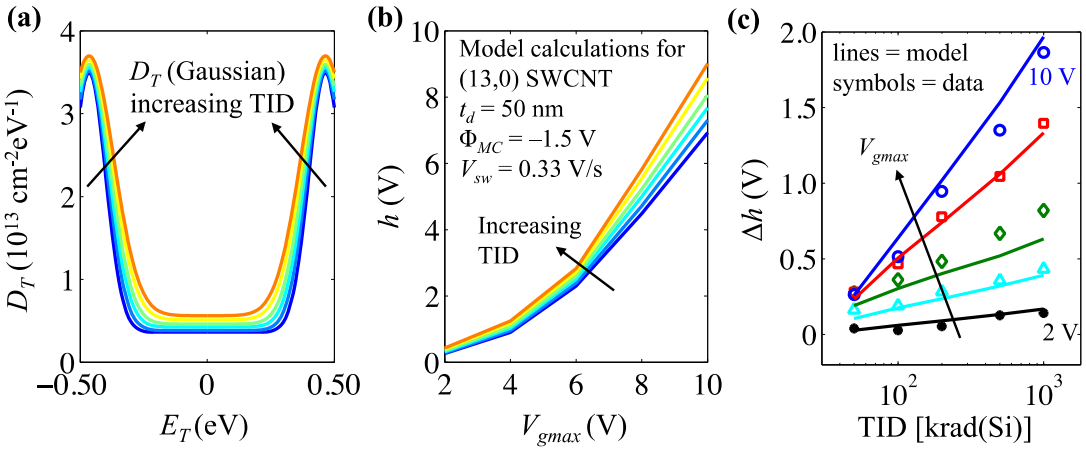

Figure 7. (a) Simulated non-uniform D_T distributions increasing with total ionizing dose (TID) [14]. (b) Model calculations of hysteresis width as a function of V_{gmax} for increasing TID [14]. (c) Comparison of simulated and measured increase in hysteresis width (h) as a function of TID and V_{gmax}. Model calculations are for a (13,0) zigzag SWCNT in an array with density of 1 nanotube/μm and t_d = 50 nm [14].

C. Oxide Trapped Charges (Aligned SWCNT FETs)

The effects of radiation-induced oxide trapped charges in aligned SWCNT FETs are investigated as part of the RadCNT program. Shown in Figs. 8a and 8b are the I_d-V_{gs} and I_d-V_{ds} curves for a back-gated aligned SWCNT FET and for increasing TID [25]. These measurements were obtained following step-stress Co-60 irradiations under static vacuum. The results in Figs. 8a and 8b reveal voltage shifts that are consistent with hole trapping near the CNTs/oxide interface. Extractions of drain conductance ($g_{ds} = \partial I_d/\partial V_{ds}$) are obtained from the I_d-V_{ds} characteristics in Fig. 8b and plotted in Fig. 9a as a function of $|V_{ds}|$ for increasing TID and for a constant $V_{gs} = -5$ V. The results in Fig. 9a indicate a reduction in g_{ds} as a function of TID consistent with increased scattering from charged impurities (i.e., oxide trapped charges) that limits mobility for low values of carrier charge density (Q_c). Drain conductance is directly proportional to the effective carrier mobility, i.e., $\mu_{eff} = (g_{ds}L)/(WQ_c)$, for FETs operating in the linear region. The results in Fig. 9a do not consider the discrepancies in Q_c that result from radiation-induced threshold shifts in the I-V characteristics. Therefore, a better characterization of increased scattering and its radiation response is obtained by plotting the low V_{ds} drain conductance (g_{ds0}) as a function of $V_{gs} - V_{th}$ (where $Q_n \propto V_{gs} - V_{th}$) as shown in Fig. 9b. For the results in Fig. 9b, V_{th} is calculated from the shifts in I_d-V_{gs} characteristics plotted in Fig. 8a. The results in Fig. 9b demonstrate the degradation of g_{ds0} as consistent with increased Coulomb scattering by radiation-induced trapped charges [25].

The results in Fig. 9b do not reveal a strong dependence of the radiation response on Q_n. In other words, the reduction in g_{ds0} as a function of TID appears comparable for all values of $V_{gs} - V_{th}$. This could indicate that for the results in Fig. 9b, the transition from Coulomb scattering limited mobility to other mechanisms is not occurring for the shown voltages, or that ionizing radiation also enhances the scattering mechanisms at large Q_n (e.g., surface roughness). However, a better experimental extraction of Q_n is required to obtain μ_{eff} and confirm these observations since using V_{th} extracted from Fig. 6a to estimate Q_n could be introducing additional discrepancies.

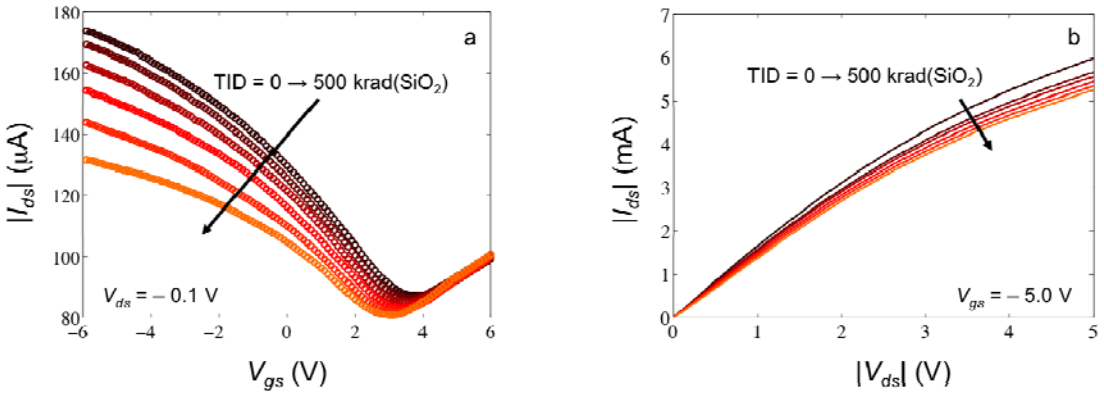

Fig. 8. (a) Transfer characteristics of a *p*-type aligned SWCNT back-gated FET for increasing total dose exposure from 0 to 500 krad(SiO_2) and for $V_{ds} = 0.1$ V [25]. (b) Output characteristics for increasing total dose exposure from 0 to 500 krad(SiO_2) and for $V_{gs} = -5.0$ V. $W = 200$ μm, $L = 2$ μm, $t_{ox} = 50$ nm (SiO_2), CNT density is ~ 1 – 2 per μm of channel width [25].

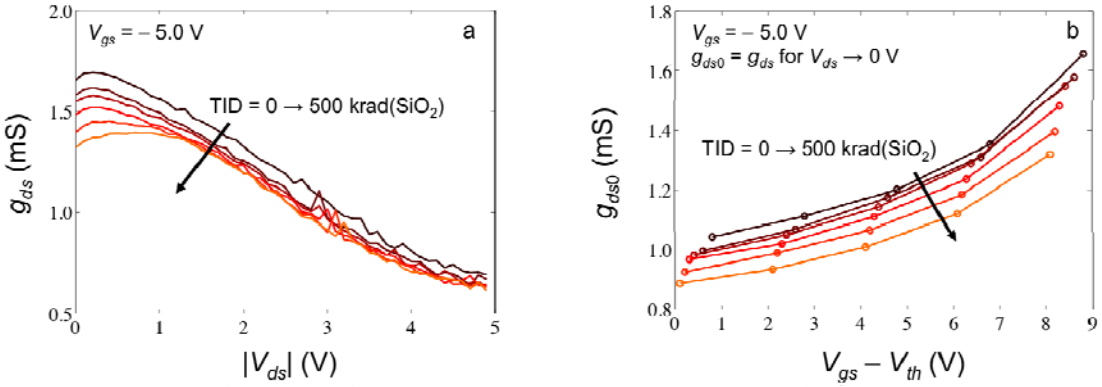

Fig. 9. (a) Drain conductance ($g_{ds} = \partial I_d/\partial V_{ds}$) plotted as a function of V_{ds} for increasing total dose exposure from 0 to 500 krad(SiO_2) and for V_{gs} = – 5.0 V [25]. (b) Low-field drain conductance ($g_{ds0} = \partial I_d/\partial V_{ds}$ for $V_{ds} \rightarrow 0$) plotted as a function of $V_{gs} - V_{th}$ for increasing total dose exposure from 0 to 500 krad(SiO_2) where V_{th} is extracted from the transfer characteristics in Fig. 8a. W = 200 µm, L = 2 µm, t_{ox} = 50 nm (SiO_2), CNT density is ~ 1 – 2 per µm of channel width [25].

D. TID Effects (Graphene FETs)

As part of the RadCNT effort, top-gated graphene FETs (GFETs) fabricated with epitaxial graphene layers grown on Si-face 6H-SiC substrates via Si sublimation were used to investigate TID effects. The top-gated GFETs were fabricated using Ti/Pt/Au source and drain contacts as well as Ti/Pt/Au metal gates over a 35 nm SiO_2 dielectric layer deposited via electron beam evaporation [26]. Two-finger GFET structures with 3 µm gate lengths (L) and various gate widths (W) were selected for total dose experiments. Electrical characterization was performed following step-stress irradiations up to a total dose of 1000 krad(Si). The characterization consisted of measuring the output characteristics (*i.e.*, I_d-V_{ds}) and the transfer characteristics (*i.e.*, I_d-V_{gs}). Shown in Fig. 10a are the I_d-V_{gs} characteristics measured using V_{ds} = 1 V. The measurements in Fig. 10a reveal negative shifts in the I-V characteristics as well as an increase in the minimum drain current ($I_{d\text{-}min}$) as a function of TID. These results indicate a buildup of N_{ot} near the SiO_2/graphene layer interface shifting the minimum conductivity gate voltage (*i.e.*, the Dirac voltage V_{Dirac}) negatively as well as increasing the minimum conductivity (σ_{min}). The rise in σ_{min} results from increased graphene channel intrinsic charge density (q_{int}) and varies with N_{ot}. Shown in Fig. 10b are the I_d-V_{ds} characteristics for V_{gs} = 0 V, –1 V and –2 V measured at the same dose levels as show in Fig. 10a. The measurements in Fig. 10b indicate an increase in I_d as a function of total dose for all values of V_{gs}, consistent with the I_d-V_{gs} response.

The radiation-induced degradation of carrier mobility is determined through calculations of μ_{eff} as a function of the effective vertical field (E_{eff}). In this case, E_{eff} is approximated as $E_{eff} = Q_{gc}/\varepsilon_{ox}$, where Q_{gc} is the graphene channel charge density given by $Q_{gc} = C_{ox}(V_{gs} - V_{Dirac}) + q_{int}$. Here, q_{int} is the graphene channel intrinsic charge density that results from charge inhomogeneity in the graphene layer typically described as electron-hole puddles that arise from the random charged impurity potential fluctuations and contribute to the non-zero minimum conductivity at the Dirac point [27-30]. Shown in Fig. 11a is g_{ds} plotted as a function of V_g for all dose levels. Calculations of μ_{eff} are plotted in Fig. 11b as a function of E_{eff} and for increasing TID. In these calculations, q_{int}

is estimated by $\sigma_{\square\square\square}/\mu_{FE}$, where μ_{FE} is the peak field effect mobility and g_{ds} is extracted for V_{ds} = 0.1 V (Fig. 11a). The results in Fig. 11b reveal a decrease in μ_{eff} with increasing total dose as can be observed at $E_{eff} \sim 1$ MV/cm. Deviations from the pre-irradiation $\mu_{eff}(E_{eff})$ characteristics are due to the increased contribution of scattering mechanisms that results from radiation-induced oxide trapped charges. The deviations from the pre-irradiation $\mu_{eff}(E_{eff})$ curve are expected to continue towards lower values of E_{eff} (*i.e.*, towards lower carrier densities $n \propto E_{eff}$) where scattering due to charged impurities is the dominant mechanism. Other scattering mechanisms such as short-range scattering dominate for large carrier densities (n) [27, 31] (*i.e.*, for large E_{eff}) and the $\mu_{eff}(E_{eff})$ characteristics converge to a universal response. In Fig. 11b this convergence appears for $E_{eff} > 2$ MV/cm.

In the approach presented here, the calculations of Q_{gc} (and E_{eff}) capture the contribution of radiation-induced oxide trapped charges through the shifts in V_{Dirac}. Therefore, this approach allows determining the radiation-induced degradation of carrier mobility in GFET devices without ambiguities introduced by voltage shifts in the I_d-V_g characteristics and the changes in $\sigma_{\square\square\square}$.

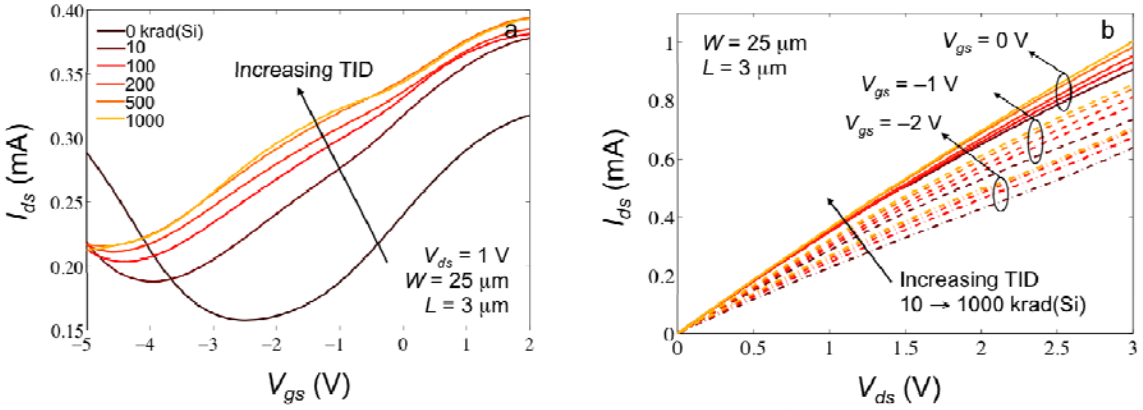

Fig. 10. (a) I_{ds} plotted as a function of V_{gs} for increasing TID up to 1000 krad(Si) for a two-finger graphene FET with W = 25 µm and L = 3 µm, V_d = 1 V and V_s = 0 V. (b) I_{ds} plotted as a function of the V_{ds} at increasing TID up to 1000 krad(Si) for V_g = 0, –1 and –2 V.

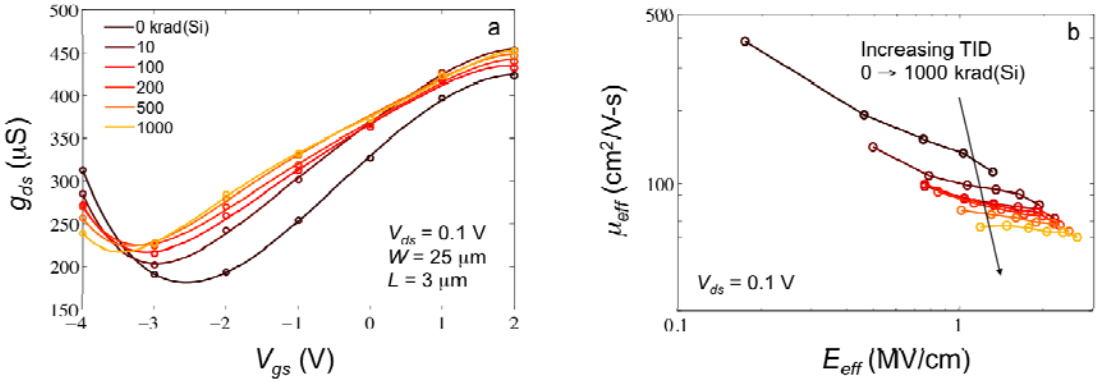

Fig. 11. (a) Drain conductance (g_{ds}) vs. V_{gs} for V_{ds} = 0.1 V and for increasing dose levels up to 1000 krad(Si). (b) Effective electron mobility (μ_{eff}) vs. effective vertical field (E_{eff}) for increasing TID up to 1000 krad(Si). The values of μ_{eff} are extracted from the g_{ds} plotted in (a).

Figure 12a shows calculations of μ_{eff} as a function of E_{eff} for increasing N_{ot} obtained as described in [19] The calculations in Figure 12a correctly describe the reduction in μ_{eff} with N_{ot} (*i.e.*, $\mu_{eff} \propto 1/N_{ot}$) for low n and the merging with the short-range scattering limited mobility μ_{SR} (dashed lined) for large n. The increase in μ_{eff} for decreasing $E_{eff} < \sim 1$ MV/cm has been previously reported in [31] and attributed to scatterer transparency occurring when carrier wavelengths exceed the spacing between scatterers. In this work, the μ_{eff} dependence to scatterer transparency in the low n limit is modeled independently from charged impurity and short-range scattering using an empirical function. Shown in Figure 12b are calculations of μ_{eff} compared with extractions from experimental data from irradiated GFETs. As shown in Figure 12b, the model calculations fit the experimental data with good qualitative agreement validating the presented approach. The modeling approach described in [19] can be directly applied to introduce radiation-induced degradation in GFET *I-V* characteristics into compact models.

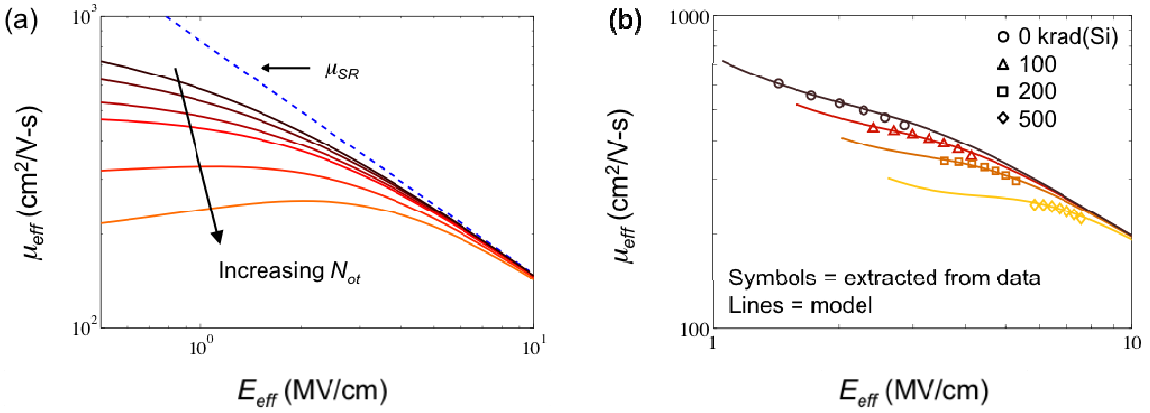

Fig. 12. Calculations of the effective electron mobility (μ_{eff}) plotted as a function of the effective vertical field (E_{eff}) for increasing values of N_{ot}. The dashed line corresponds to short-range mobility (b) Comparison of μ_{eff} extracted from data and model calculations (lines) including scatterer transparency.

V. FUTURE WORK

1. TID experiments using T-gate and/or aluminum top-gated SWCNT FETs with reduced gate hysteresis.
    - Development of mostly semiconducting aligned SWCNT devices with reasonable (~10^4) I_{on}/I_{off} ratios making use of different dielectric materials, passivation layers and processing steps to achieve significant mitigation of gate hysteresis. The use of controlled breakdown techniques for removal of metallic tubes and/or chirality-controlled synthesis of SWCNT to obtain the desired I_{on}/I_{off} ratios will also be demonstrated. TID effects will be verified in devices with reduced gate hysteresis and high I_{on}/I_{off} ratios.
2. TID experiments on CMOS gates and basic circuits with aligned SWCNT FETs.
    - Fabrication of p-type and n-type aligned SWCNT FETs with different gate configurations (i.e., front and/or back-gated), various gate dielectric materials and thicknesses and different passivation layers. Development of simple CMOS logic gates such as NAND, NOR and INV. This task will also include pre-irradiation characterization of the test structures to demonstrate the electrical performance, reliability and variation of the transistors and logic gate structures
3. TCAD simulation of aligned SWCNT FET devices including radiation-induced degradation due to oxide trapped charges.
    - Development of particle-based Monte Carlo simulator (Boltzmann transport theory including Coulomb scattering from oxide trapped charges) coupled with Poisson solver.

VI. PARTICIPATING & OTHER COLLABORATING ORGANIZATIONS

1. **Naval Research Laboratory**
   Washington DC
   Dr. Cory Cress
   Materials Research Engineer
   Solid State Devices Branch
   cory.cress@nrl.navy.mil
   TASK: Radiation testing

2. **SILVACO International**
   San Diego, CA
   Mark Maurer
   Director, Government Business Div.
   mark.maurer@silvaco.com
   TASK: TCAD tools for CNT simulation

3. **Hughes Research Laboratory (HRL)**
   Jeong-Sun Moon
   Project Leader
   jmoon@hrl.com
   TASK: Graphene FET (SiC) sample fabrication

4. **University of Texas at Austin**
   Prof. Rodney Ruoff
   r.ruoff@mail.utexas.edu
   TASK: Graphene FET (CVD) sample fabrication

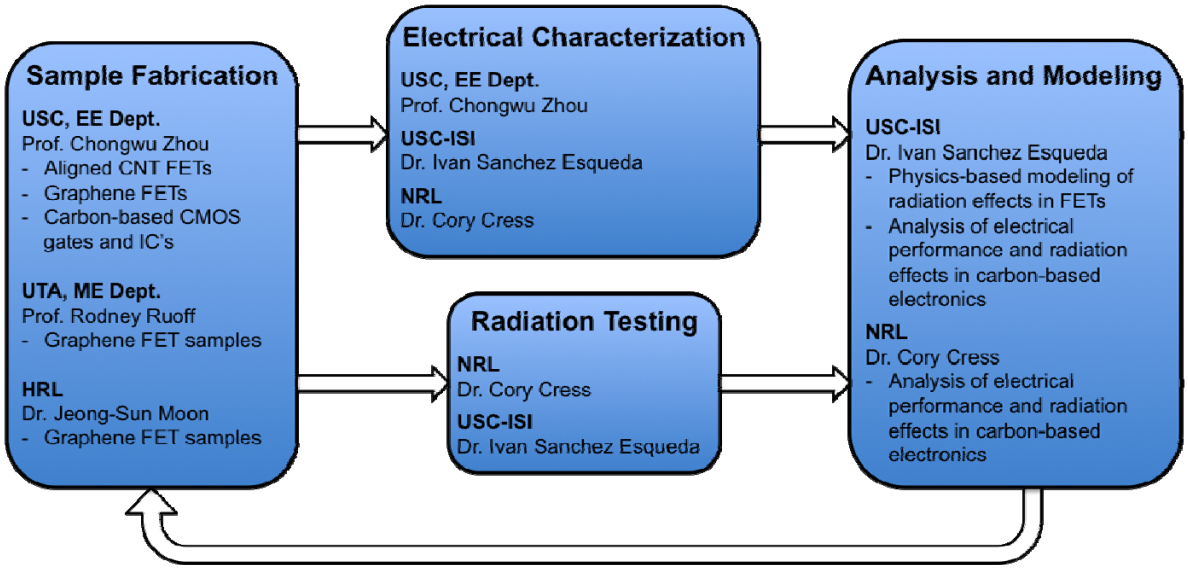

Fig. 10. Flow diagram of RadCNT program collaborations.

VII. IMPACT

Understanding the fundamental mechanisms of radiation interaction with carbon-based electronics including nanotube and graphene based transistors is an important enabler for key applications of DTRA interest. The small (molecular) size of carbon nanotubes and graphene together with their very strong carbon-carbon covalent bonds make this material system of interest for radiation hard applications. In addition, carbon electronics has the potential for low power operation and highly linear amplification that are also of key interest for critical space applications in harsh radiation environments. Graphene is of particular interest for low power RF components including LNA's, Mixers, etc. Carbon electronics may also turn out to be of interest for robust operations in non-space radiation environments such as radiation sensors, etc. High impact accomplishments of the RadCNT program are:

- Multiple publications and talks at major radiation effects conferences including NSREC, RADECS and GOMAC.

- Transferable physics-based TCAD models that can be incorporated into commercial (e.g., SILVACO) tools for modeling TID effects of SWCNT and graphene FETs are being developed.
- Fabrication processes for SWCNT and graphene FETs with improved electrical performance and little to no hysteresis effects are being developed.
- Several sets of TID radiation data have been obtained for both SWCNT and graphene FETs in collaboration with NRL.

VIII. PERSONNEL SUPPORTED

USC-ISI, Faculty: Prof. Michael Fritze, Prof. John Granacki
Researchers: Dr. Ivan Sanchez Esqueda, Dr. Jon Ahlbin, Dr. Younes Boulghassoul
Students: Stephanie Weeden-Wright (Student Intern)

USC-EE, Faculty: Prof. Chongwu Zhou
Students: Jialu Zhang, Yue Fu, Pyojae Kim

NRL-SSD, Researcher: Dr. Cory Cress.

IX. PRESENTATION, TALKS AND COURSES

1. I. S. Esqueda, C. D. Cress, Y. Cao, Y. Che, and C. Zhou, " Radiation-induced degradation of transport in nanoscale transistors," *to be presented at IEEE Nuclear and Space Radiation Effects Conference (NSREC)*, July 2014.
2. I. S. Esqueda, C. D. Cress, Y. Che, Y. Cao and C. Zhou, "Charge trapping in aligned single-walled carbon nanotube arrays induced by ionizing radiation exposure," *Journal of Applied Physics*, 115, 054506, 2014.
3. I. S. Esqueda, C. D. Cress, T. J. Anderson, J. R. Ahlbin, M. Bajura, M. Fritze and J. S. Moon, "Modeling radiation-induced degradation in top-gated epitaxial graphene field-effect transistors (FETs)," Electronics, no. 2, pp. 234-245, 2013.
4. I. S. Esqueda, Y. Fu, C. D. Cress, J. Zhang, C. Zhou, J. Ahlbin, M. Bajura, G. Boverman, M. Fritze, "Modeling the Effect of Hysteresis on Aligned Nanotube FETs Exposed to Ionizing Radiation," *2012 IEEE RADECS conference proceedings*.
5. J. R. Ahlbin, I. S. Esqueda, C. D. Cress, P. J. McMarr, H. L. Hughes, Fellow, IEEE, Y. Fu, J. Zhang, C. Wang, C. Zhou, M. Bajura, G. Boverman, and M. Fritze, "Total Dose Effects in Aligned Carbon Nanotube Transistors with Al2O3 Gate Dielectrics," *2012 IEEE RADECS conference proceedings*.
6. A. Badmaev, Y. Che, Z. Li, C. Wang and C. Zhou "Self-aligned fabrication of graphene transistors with T-shaped gate," *presented at APS March meeting 2012*.
7. Y. Che, C. Wang, J. Liu, X. Lin, H.-S. P. Wong and C. Zhou, "Selective Synthesis and Device Applications of Semiconducting Single-Walled Carbon Nanotubes Using Isopropanol as Feedstock," *presented at APS March meeting 2012*.
8. Y. Fu, J. Zhang, C. Wang, C. Zhou, R. Wormuth, V. Tyree, M. Fritze, P. McMarr, and H. Hughes, "Total Dose Radiation Effects in Carbon Nanotube Transistors,"

2011 GOMACTech Proceedings.

9. J. Liu, C. Wang, X. Tu, B. Liu, L. Chen, M. Zheng, and C. Zhou, "Chirality-controlled synthesis of single-wall carbon nanotubes using vapour-phase epitaxy," *Nature communications,* vol. 3, p. 1199, 2012
10. Y. Che, A. Badmaev, A. Jooyaie, T. Wu, J. Zhang, C. Wang, K. Galatsis, H. A. Enaya, and C. Zhou, "Self-Aligned T-Gate High-Purity Semiconducting Carbon Nanotube RF Transistors Operated in Quasi-Ballistic Transport and Quantum Capacitance Regime". *ACS Nano, Article ASAP 2012*.
11. Y. Che, C. Wang, J. Liu, B. Liu, X. Lin, J. Parker, C. Beasley, H. S. P. Wong, and C. Zhou, "Selective Synthesis and Device Applications of Semiconducting Single-Walled Carbon Nanotubes Using Isopropyl Alcohol as Feedstock," *ACS Nano,* vol. 6, pp. 7454-7462, 2012/08/28 2012.
12. Wang, K. M. Ryu, A. Badmaev, J. Zhang, and C. Zhou, "Metal Contact Engineering and Registration-Free Fabrication of Complementary Metal-Oxide Semiconductor Integrated Circuits Using Aligned Carbon Nanotubes," *ACS Nano,* vol. 5, pp. 1147-1153, Feb 2011.
13. C. D. Cress, J. G. Champlain, I. S. Esqueda, J. T. Robinson, A. L. Friedman and J. J. McMorrow, "Total Ionizing Dose Induced Charge Carrier Scattering in Graphene Devices*," IEEE Trans. Nucl. Sci.*, vol. 29, no. 6, Dec. 2012.

Courses Taught: Prof. Chongwu Zhou (USC EE Dept)
EE480: Introduction to Nanoscience and Nanotechnology

X. REFERENCES

[1] C. D. Cress, J. J. McMorrow, J. T. Robinson, A. L. Friedman, and B. J. Landi, "Radiation effects in single-walled carbon nanotube thin-filmtransistors," *IEEE Trans. Nucl. Sci.*, vol. 57, no. 6, pt. 1, pp. 3040–3045, Dec. 2010.

[2] Y. Fu, J. Zhang, C. Wang, C. Zhou, R. Wormuth, V. Tyree, M. Fritze, P. McMarr, and H. Hughes, "Total Dose Radiation Effects in Carbon Nanotube Transistors," *GOMACTech 2011 Proceedings*, 2011.

[3] E. X. Zhang, A. K. Newaz, B. Wang, S. Bhandaru, C. Xuan Zhang, D. M. Fleetwood, K. I. Bolotin, S. T. Pantelides, M. L. Alles, R. D. Schrimpf, S. M. Weiss, R. A. Reed and R. A. Weller, "Low-energy X-ray and ozone-exposure induced defect formation in graphene materials and devices," *IEEE Trans. Nucl. Sci.*, vol. 58, pp. 2961-2967, Dec. 2011.

[4] C. D. Cress, J. J. McMorrow, J. T. Robinson, B. J. Landi, S. M. Hubbard and S. R. Messenger, "Radiation Effects in Carbon Nanoelectronics," *Electronics*, vol. 1, no. 1, pp. 23-31 Sep. 2012.

[5] H. Mai-Xing, J. Zhuo-Yu, S. Li-Wei, C. Ying-Ping, W. Hong, L. Xin, L. Dong-Mei and L. Ming. "Gamma radiation caused graphene defects and increased carrier density," *Chin. Phys. B.*, vol. 20, no. 8, 086102, 2011.

[6] J. R. Ahlbin, I. S. Esqueda, C. D. Cress, S. L. Weeden-Wright, P. J. McMarr, H. L. Hughes, A. L. Friedman, Y. Fu, J. Zhang, C. Wang, C. Zhou, M. Bajura, G. Boverman and M. Fritze, "Total Dose Effects in Aligned Carbon Nanotube Transistors with Al_2O_3 Gate Dielectrics," *Proceedings of the 2012 IEEE RADECS conference*.

[7] H. Hongo, F. Nihey, and S. Yorozu, "Relationship between carbon nanotube density and hysteresis characteristics of carbon nanotube random network-channel field effect transistors," *Journal of Applied Physics*, vol. 107, no. 9, p. 094501, 2010.

[8] W. Kim, A. Javey, O. Vermesh, Q. Wang, Y. Li, and H. Dai, "Hysteresis Caused by Water Molecules in Carbon Nanotube Field-Effect Transistors," *Nano Letters*, vol. 3, no. 2, pp. 193-198, Feb. 2003.

[9] K. Bradley, J. Cumings, A. Star, and J.-C. P. Gabriel and G. Grüner, "Influence of Mobile Ions on Nanotube Based FET Devices," *Nano Letters*, vol. 3, no. 5, pp. 639-641, 2003.

[10] A. Robert-Peillard and S. V. Rotkin, "Modeling Hysteresis Phenomena in Nanotube Field-Effect Transistors," *IEEE Transactions On Nanotechnology*, vol. 4, no. 2, pp. 284-288, Mar. 2005.

[11] A. Vijayaraghavan, S. Kar, C. Soldano, S. Talapatra, O. Nalamasu, and P. M. Ajayan, "Charge-injection-induced dynamic screening and origin of hysteresis in field-modulated transport in single-wall carbon nanotubes," *Applied Physics Letters*, vol. 89, no. 16, p. 162108, 2006.

[12] H. Shimauchi, Y. Ohno, S. Kishimoto, and T. Mizutani, "Suppression of Hysteresis in Carbon Nanotube Field-Effect Transistors: Effect of Contamination Induced by Device Fabrication Process," *Japanese Journal of Applied Physics*, vol. 45, no. 6B, pp. 5501-5503, Jun. 2006.

[13] I. S. Esqueda, Y. Fu, C. D. Cress, J. Zhang, C. Zhou, J. Ahlbin, M. Bajura, G. Boverman and M. Fritze, "Modeling the Effect of Hysteresis on Aligned Nanotube FETs Exposed to Ionizing Radiation," *Proceedings of the 2012 RADECS conference*

[14] I. S. Esqueda, C. D. Cress, Y. Che, Y. Cao and C. Zhou, "Charge trapping in aligned single-walled carbon nanotube arrays induced by ionizing radiation exposure," *Journal of Applied Physics*, 115, 054506, 2014.

[15] G. Buchowicz, P. R. Stone, J. T. Robinson, C. D. Cress, J. W. Beeman and O. D. Dubon, "Correlation between structure and electrical transport in ion-irradiated graphene grown on Cu foils," *Applied Physics Letters*, Vol. 98, pp. 032102, 2011.

[16] I. S. Esqueda, C. D. Cress, Y. Cao, Y. Che, and C. Zhou, " Radiation-induced degradation of transport in nanoscale transistors," *to be presented at IEEE Nuclear and Space Radiation Effects Conference (NSREC)*, July 2014.

[17] C. D. Cress, J. G. Champlain, I. S. Esqueda, J. T. Robinson, A. L. Friedman and J. J. McMorrow, "Total Ionizing Dose Induced Charge Carrier Scattering in Graphene Devices*," IEEE Trans. Nucl. Sci.*, vol. 29, no. 6, Dec. 2012.

[18] I. S. Esqueda, C. D. Cress, T. J. Anderson, J. R. Ahlbin, M. Bajura, M. Fritze, J.-S. Moon, "Modeling Radiation-Induced Degradation in Top-Gated Epitaxial Graphene FETs," *Presented at the 2012 IEEE NSREC conference*, 2012.

[19] I. S. Esqueda, C. D. Cress, T. J. Anderson, J. R. Ahlbin, M. Bajura, M. Fritze and J. S. Moon, "Modeling radiation-induced degradation in top-gated epitaxial graphene field-effect transistors (FETs)," Electronics, no. 2, pp. 234-245, 2013.

[20] C. Wang, K. Ryu, L. G. Arco, A. Badmaev, J. Zhang, X. Lin, Y. Che, and C. Zhou, "Synthesis and device applications of high-density aligned carbon nanotubes using low-pressure chemical vapor deposition and stacked multiple transfer," *Nano Research,* vol. 3, pp. 831-842, 2010.

[21] Y. Che, C. Wang, J. Liu, B. Liu, X. Lin, J. Parker, C. Beasley, H. S. P. Wong, and C. Zhou, "Selective Synthesis and Device Applications of Semiconducting Single-Walled Carbon Nanotubes Using Isopropyl Alcohol as Feedstock," *ACS nano,* vol. 6, pp. 7454-7462, 2012/08/28 2012.

[22] J. Liu, C. Wang, X. Tu, B. Liu, L. Chen, M. Zheng, and C. Zhou, "Chirality-controlled synthesis of single-wall carbon nanotubes using vapour-phase epitaxy," *Nature communications,* vol. 3, p. 1199, 2012.

[23] Y. Che, A. Badmaev, A. Jooyaie, T. Wu, J. Zhang, C. Wang, K. Galatsis, H. A. Enaya, and C. Zhou, "Self-Aligned T-Gate High-Purity Semiconducting Carbon Nanotube RF Transistors Operated in Quasi-Ballistic Transport and Quantum Capacitance Regime," *ACS nano,* vol. 6, pp. 6936-6943, Aug 2012.

[24] C. Wang, K. M. Ryu, A. Badmaev, J. Zhang, and C. Zhou, "Metal Contact Engineering and Registration-Free Fabrication of Complementary Metal-Oxide Semiconductor Integrated Circuits Using Aligned Carbon Nanotubes," *ACS nano,* vol. 5, pp. 1147-1153, Feb 2011.

[25] I. S. Esqueda, *unpublished work*, 2013.

[26] J. S. Moon, D. Curtis, S. Bui, M. Hu, D. K. Gaskill, J. L. Tedesco, P. Asbeck, G. G. Jernigan, B. L. VanMil, R. L. Myers-Ward, C. R. Eddy, P. M. Campbell and X. Weng, "Top-gated epitaxial graphene FETs on Si-Face SiC wafers with a peak transconductance of 600 mS/mm," *IEEE Electron Device Letters*, vol. 31, no. 4, pp. 260-262, Apr. 2010.

[27] T. O. Wehling, E. Şaşıoğlu, C. Friedrich, A. I. Lichtenstein, M. I. Katsnelson and S. Blügel, "Strength of Effective Coulomb Interactions in Graphene and Graphite," *Physical Review Letters*, vol. 106, no. 23 p. 236805, Jun. 2011.

[28] J. Martin, N. Akerman, G. Ulbricht, T. Lohmann, J. H. Smet, K. Von Klitzing and A. Yacoby. "Observation of electron-hole puddles in graphene using a scanning single-electron transistor," *Nature Phys.*, vol. 4, pp. 144-148, Feb. 2008.

[29] J.-H. Chen, W. G. Cullen, C. Jang, M. S. Fuhrer and E. D. Williams "Defect scattering in graphene." *Physical Review Letters*, vol. 102, no. 24, p. 236805, Jun. 2009.

[30] S. Adam, E. H. Hwang, V. M. Galitski and S. Das Sarma, “A self-consistent theory for graphene transport,” *Proc. Natl Acad. Sci. USA*, vol. 104, no. 47, pp. 18392-18397, Nov. 2007.

[31] D. B. Farmer, V. Perebeinos, Y-M. Ling, C. Dimitrakopoulos and P. Avouris, “Charge trapping and scattering in epitaxial graphene,” *Phys. Rev. B*, vol. 84, no. 20, pp. 205417, Nov. 2011.

Department Of Defense

Defense Technical Information Center
8725 John J. Kingman Road, Suite 0944
Ft. Belvoir, VA 22060-6201
ATTN: DTIC/OCA

Defense Threat Reduction Information Analysis
Center 8725 John J. Kingman Road, Suite 0944
Ft. Belvoir, VA 22060-6201
ATTN: DTRIAC

Defense Threat Reduction Agency
8725 John J. Kingman Road
Ft. Belvoir, VA 22060-6201
ATTN: Jacob Calkins